Computation of Near-Field Microwave Radiometric Signals: Definition and Experimental Verification

Ahmed Mamouni, Yves Leroy, Bertrand Bocquet, J. C. van de Velde, and Philippe Gelin, *Associate Member, IEEE*

Abstract—**Applications of microwave radiometry for thermometry of bulk materials require the development of methods of computation of the radiometric signals. Owing to the reciprocity theorem, the radiometric signals can be deduced from a knowledge of the near field radiated in the assumed lossy material by the antenna which is being used as a probe in the radiometric operation. In this paper, we propose a modal method for computing the field. This method has first been tested in an active process by measurements of the radiated field. It also gives excellent agreement with experimental data obtained in the bands around 1.5 and 3 GHz over a lossy material (water) in both total power and correlation radiometry.**

I. Introduction

MICROWAVE radiometry is being used in order to measure the near-field thermal noise transmitted by lossy materials in the microwave frequency range. This noninvasive method is of interest for medical investigations. Because of the moderate absorbtion of living tissue and the temperature gradients which occur in the human body, it is now acknowledged that this technique is able to provide information about the temperatures in tissue to depths of several centimeters. As a matter of fact, studies have been carried out on the construction of systems devoted to applications such as total power radiometers [1]–[5], radiometric imaging [6], and correlation radiometers [7]–[11]. Several works have already shown the potential of such techniques for diagnostic applications [1], [3], [4], [12], for the control of hyperthermia [13]–[15], and for other thermological applications [16]. Attempts are also being made to deduce the temperature distribution in the volume submitted to radiometric investigations [5], [17]–[19]. Before working out the problem of inversion, we need to solve the direct problem, i.e., to compute the radiometric signals in order to forecast the influence of the nature of the material, the size, the depth and the shape of the thermal structures, as well as the characteristics of the probe and frequency. A method of computation is also needed in order to define the data processing compatible with a significant positioning of multiprobes and data processing in the synthesis of radiometric images.

In this paper we first recall that the computation of radiometric signals requires a knowledge of the field transmitted by the antenna (or probe) at any point in the lossy material under test. After surveying other works in this field, we present our work, which is based on a modal method of determining the near field transmitted in a lossy material by means of a rectangular waveguide aperture. The principle of this method is discussed, and its results are verified by experiments both in an active process (when the antenna transmits a signal toward the material) and in a passive process (when the antenna receives the thermal noise transmitted by the different subvolumes of the material). The radiometric data concern both total power radiometry and correlation radiometry.

II. Principle of Computing Radiometric Signals

We first consider the case of a total power radiometer, or, what is always achieved in practice, a Dicke radiometer [20], which reduces to an analogous situation. In this case (Fig. 1), the output signal is proportional to the noise power received by the probe, or antenna, placed flush on the material under test. According to the fluctuation–dissipation theorem [21], the spontaneous movements of electrical particles and dipole moments of the material create random electric and magnetic fields $\zeta_i(t)$ and $h_i(t)$ while these fields create electromagnetic noise signals which are received by the probe. Taking into account the incoherent character of these signals (thermal noise), the total field $E(t,f)$ received by the probe in a small bandwidth around the frequency f is the sum of electromagnetic signals transmitted by the different subvolumes called ΔV_i. In this way,

$$E(t,f) = \sum_{i=1}^{\infty} a_i(f)\zeta_i(t) \tag{1}$$

with $a_i(f)$ a parameter describing the coupling between the probe and ΔV_i. Consequently, the output signal of the radiometer becomes

$$S(f) = G(f)\langle E^2(t,f)\rangle = G(f)\sum_{i=1}^{\infty} a_i^2(f)\langle \zeta_i^2(t)\rangle \tag{2}$$

Manuscript received August 16, 1989; revised July 5, 1990. This work was supported by the Agence National pour la Valorisation de la Recherche (ANVAR), the Etablissement publique Régional Nord Pas de Calais, and the Ministère de la Recherche et de la Technologie (France).

The authors are with the Centre Hyperfréquences et Semiconducteurs, Université des Sciences et Techniques de Lille Flandres Artois, France.

IEEE Log Number 9040551.

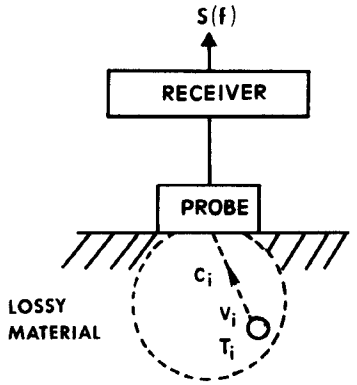

Fig. 1. Origin of the radiometric signals in the case of a classical radiometer.

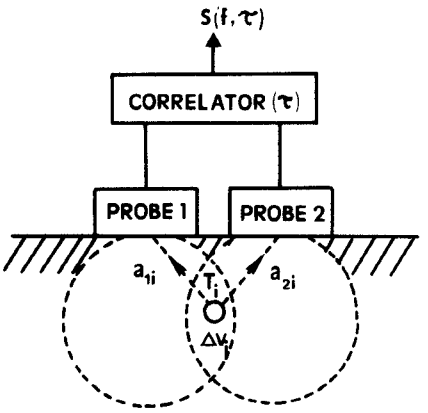

Fig. 2. Origin of the radiometric signals in the case of a correlation radiometer.

with $G(f)$ the transmittance (or power gain) of the receiver at the frequency f. According to the dissipation–fluctuation theorem, $\langle \zeta_i^2(t) \rangle$ is proportional to the local absolute temperature T_i in ΔV_i. Consequently,

$$S(f) = G(f) \sum_{i=1}^{\infty} C_i(f) T_i \tag{3}$$

where

$$C_i(f) = a_i^2(f) \tag{4}$$

or the weighting function of ΔV_i with respect to the probe.

In other words, let us consider the situation described in Fig. 1, in which the receiver is a matched load, and the whole system is at thermodynamic equilibrium. The part of the noise power emitted by the matched load, for a limited bandwidth Δf, around a frequency f, which is dissipated in a subvolume ΔV_i of the lossy material, is necessarily equal to the noise power transmitted from ΔV_i to the matched load through the probe. Indeed, this proposition must be achieved in order to agree with the second principle of thermodynamics, which asserts that the whole system must continue to be at thermal equilibrium. Moreover, the matched load associated with the probe and the subvolume ΔV_i can be considered as two antennas, for which the reciprocity theorem applies. This process occurs in the same way for the different bandwidths Δf in terms of the principle of detailed balancing [22].

Consequently, the radiometric signal can be expressed in terms of an excess of radiometric temperature ΔT_m with respect to the reference temperature T_0, i.e.,

$$\Delta T_m = \sum_{i=1}^{\infty} C_i \Delta T_i \tag{5}$$

with

$$T_i = T_0 + \Delta T_i. \tag{6}$$

According to the principle of detailed balancing and the reciprocity theorem, we have

$$a_i(f) = K_1 E_i(f) \tag{7}$$

or

$$C_i = K_2 \sigma_i E_i^2(f) \tag{8}$$

with σ_i and $E_i(f)$ being the conductivity of the material and the electric field radiated at ΔV_i by the probe when transmitting a monochromatic signal at f. The parameters K_1 and K_2 can easily be determined because in the case of a material at uniform temperature $T_0 + \Delta T$ we have

$$\Delta T_m = \Delta T\left(1 - |\rho|^2\right) \tag{9}$$

where ρ is the voltage reflection coefficient at the probe–material interface. As a matter of fact, relation (3) has to be integrated over the bandwidth of the radiometer.

In conclusion, as a consequence of relations (7) and (8), we stress that computation of radiometric signals requires a knowledge of the field distribution radiated in the material in the active process.

A correlation radiometer works in a different manner. In this kind of system (Fig. 2) two probes, put for example flush on the lossy material under test, are connected to a microwave correlator [7]. This system reduces to an analog microwave multiplier connected to a delay line (which produces the delay time of the correlator) and followed by an integrator.

The previous reasoning about the transmission of thermal noise signals is applied here again. In this way, the new expression of the coupling of the system to a subvolume ΔV_i, for a small bandwidth around the frequency f, becomes

$$C_i'(f,\tau) = a_{1i}(f,t) \cdot a_{2i}^*(f, t+\tau) \tag{10}$$

where $a_{ji}(f)$ is the term as defined by relations (1), (2), (7), and (8) with respect to the probe j, τ is the delay time considered and the asterisk denotes complex conjugate. Hence

$$C_i'(f,\tau) = K_3 \sigma_i(f) E_{1i}(f,t) \cdot E_{2i}^*(f, t+\tau) \Delta V_i \tag{11}$$

where $E_{1i}(f,t)$ and $E_{2i}(f,t)$ are the fields created in ΔV_i when the antennas j ($j = 1$ or 2) are active and fed by the same monochromatic generator at the frequency f. K_3 is a calibration factor.

Relation (11) can also be written as [7]

$$C_i'(f,\tau) = K_3 \sigma_i(f) |E_{1i}(f)| \cdot |E_{2i}(f)| \cos\left(\Phi_{1i} - \Phi_{2i} - \Delta\Phi\right) \cdot \cos\Psi \Delta V_i \tag{12}$$

where Φ_{1i} and Φ_{2i} are the phase shifts relative to the fields radiated in ΔV_i by the two probes, Ψ is the angle between the orientation of the fields $E_{1i}(f)$ and $E_{2i}(f)$, and $\Delta\Phi$ is $2\Pi f\tau$ or the phase shift introduced by the delay time τ.

As a matter of fact, this process defines a synthetic aperture antenna with weighting functions which depend on a greater number of parameters than in total power radiometer. The output signal of the system, however, is given in a form similar to that of the total power radiometer, i.e.,

$$S(f,\tau) = G'(f) \sum_{i=1}^{\infty} C_i'(f,\tau) T_i \tag{13}$$

where $G'(f)$ is the transmittance of the correlator. In other words, the radiometric signal is expressed in terms of a radiometric temperature:

$$\Delta T_m = \sum_{i=1}^{\infty} C_i' \Delta T_i. \tag{14}$$

Here also relations such as (13) and (14) have to be integrated over the bandwidth of the system.

III. Computation of the Field Radiated in the Active Process

We consider next the case of the field radiated by the aperture of a monomode rectangular waveguide in a semi-infinite homogeneous lossy material. The determination of the electric field in three dimensions requires us to consider the discontinuity between the two media, taking into account the mode matching technique of the transverse fields. The rigorous processing requires very complex methods and prohibitive computation times. Consequently, approximations are often needed which depend on the formulation of the problem. Several authors have considered this approach, mainly in the modeling of applicators for therapeutic hyperthermia or probes for radiometry.

Guy [24] has studied the dosimetry of electromagnetic radiation for research concerning biological effects. Considering the same structure as reported here, he employed a spectral approach deduced from the Fourier transform such as that proposed by Villeneuve and Harrington [25], [26]. Bardati *et al.* [27] used a multimode two-dimensional model, which is the basis for a multispectral temperature retrieval method. Cheever *et al.* [28] started from the mode matching technique as described by Harrington in order to compute the penetration depth along the axis of the structure (distance over which the power density is reduced by a factor $1/e$). Bolomey *et al.* [29] and Rebollar *et al.* [30] studied the model of a junction between a monomode waveguide and an oversized waveguide filled with lossy material. An integral representation of the fields at the discontinuity between the two waveguides leads to the solution of systems of linear equations in matrix form (moment method). In order to cancel the influence of the walls of the second waveguide, it is necessary to consider an important ratio between the dimensions of the waveguide, leading to a matrix which occupies a memory of large size in the computer. Because of this drawback, other authors are rather reticent about this type of method [28]–[34].

For this reason, we have chosen a more realistic model of a waveguide aperture actually in contact with a semi-infinite lossy material. Moreover, our solution includes an analytical calculation associated with an iterative method, which avoids the processing of a large size matrix.

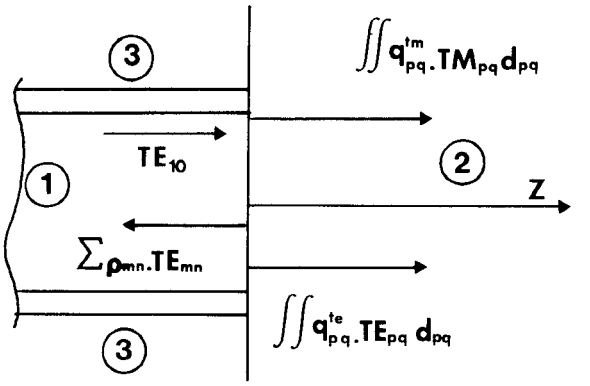

Fig. 3. Modeling of the near field radiated by the aperture of the rectangular waveguide (dimension $a \times b$) filled with a solid dielectric (medium 1: ϵ_1, μ_0) in an homogeneous lossy material (medium 2: $\epsilon_2^* = \epsilon_2' - j\epsilon_2''$; $\sigma_2 = \epsilon_0 \epsilon_2'' \omega$). Medium 3 surrounding the waveguide is free space (air) (ϵ_0, μ_0).

Analysis

Consider the structure shown in Fig. 3, which includes a rectangular waveguide filled with a dielectric (ϵ_1, μ_0), and an aperture in contact with a homogeneous, isotropic, semi-infinite lossy material of complex permittivity $\epsilon_2^* = \epsilon_2' - j\epsilon_2''$ (conductivity $\sigma_2 = \epsilon_0 \epsilon_2'' \omega$).

The propagation equations of the electromagnetic structures are

$$\left[\Delta + \Gamma_i^2\right] \begin{bmatrix} Ez \\ Hz \end{bmatrix} = 0 \tag{15}$$

where i equals 1 in the waveguide and 2 in the lossy material. Taking into account the boundary conditions, the characteristic equations in mediums 1 and 2 are as follows.

For medium 1,

$$\Gamma_1^2 = k_x^2 + k_y^2 = k_0^2 \epsilon_1 - \beta_1^2 = (2m+1)^2 \frac{\pi^2}{a^2} + 4n^2 \frac{\pi^2}{b^2} \tag{16}$$

where m and $n \in N$, a and b are the dimensions of the waveguide, and k_x and k_y are the transverse wavenumbers. Consequently, we solve for the phase constant:

$$\beta_1 = \left[k_0^2 \epsilon_1 - (2m+1)^2 \frac{\pi^2}{a^2} - 4n^2 \frac{\pi^2}{b^2} \right]^{1/2}. \tag{17}$$

For medium 2,

$$\Gamma_2^2(p,q) = k_0^2 \epsilon_2^* - \gamma_2^2(p,q) \tag{18}$$

with

$$\gamma_2^2(p,q) = \beta_2(p,q) - j\alpha_2(p,q) \tag{19}$$

being the propagation constant. Thus, the continuous modes in medium 2 are defined by three parameters: p, q (the real transverse wavenumbers), and $\gamma_2(p,q)$. These quantities are bound by the following relation:

$$p^2 + q^2 + \gamma_2^2(p,q) = k_0^2 \epsilon_2^*. \tag{20}$$

From (18), (19), and (20) we can deduce the phase constant $\beta_2(p,q)$ and the attenuation constant $\alpha_2(p,q)$ of the propa-

gating modes, i.e.,

$$\beta_2^2(p,q)=\frac{1}{2}\left\{k_0^2\epsilon_2'-p^2-q^2+\left[\left(k_0^2\epsilon_2'-p^2-q^2\right)^2+k_0^4\epsilon_2''^2\right]^{1/2}\right\} \quad (21)$$

$$\alpha_2(p,q)=k_0^2\epsilon_2''/2\beta_2(p,q) \quad (22)$$

where $k_0^2=\omega_0^2\epsilon_0\mu_0$.

As p and q can assume all values, $\beta_2(p,q)$ can also assume an infinite number of values. Consequently we have to consider a continuous spectrum of modes. In our particular situation, taking into account the fact that the second medium is lossy, and the existence of a gradient of refractive index between mediums 2 and 3 (surrounding the waveguide), we can assume that no backward continuous mode propagates in medium 3 [31].

1) Continuity Equations: Study of the discontinuity between the waveguide aperture and the lossy material leads to relations, in the corresponding plane, between all the existing modes (technique of mode matching) [26]. Thus we consider the continuity of all the tangential components of the electromagnetic fields in this plane. The expression of these continuity conditions requires first a knowledge of all the modes on both sides of the discontinuity. The continuity equations in our problem are

$$E^{10}\begin{Bmatrix}x\\y\end{Bmatrix}(1+\rho_{10})+\sum\rho_{mn}E^{te}\begin{Bmatrix}x\\y\end{Bmatrix}(mn)=\int\int_0^\infty\left[q^{te}(pq)E^{te}\begin{Bmatrix}x\\y\end{Bmatrix}(pq)+q^{tm}(pq)E^{tm}\begin{Bmatrix}x\\y\end{Bmatrix}(pq)\right]dp\,dq \quad (23)$$

$$H^{10}\begin{Bmatrix}x\\y\end{Bmatrix}(1-\rho_{10})-\sum\rho_{mn}H^{te}\begin{Bmatrix}x\\y\end{Bmatrix}(mn)=\int\int_0^\infty\left[q^{te}(pq)H^{te}\begin{Bmatrix}x\\y\end{Bmatrix}(pq)+q^{tm}(pq)H^{tm}\begin{Bmatrix}x\\y\end{Bmatrix}(pq)\right]dp\,dq. \quad (24)$$

In these expressions, the total field in the waveguide is the sum of the fields associated with the incident TE_{10} mode and higher discrete TE_{mn} modes reflected by the discontinuity while ρ_{10} and ρ_{mn} are the coupling functions associated with these modes. The quantities $q^{te}(p,q)$ and $q^{tm}(p,q)$ are, respectively, the coupling functions of the transmitted continuous modes:

$$E^{te}\begin{Bmatrix}x\\y\end{Bmatrix}(pq),H^{te}\begin{Bmatrix}x\\y\end{Bmatrix}(pq)$$

$$E^{tm}\begin{Bmatrix}x\\y\end{Bmatrix}(pq),H^{tm}\begin{Bmatrix}x\\y\end{Bmatrix}(pq).$$

2) Coupling Functions: The characterization of the discontinuity consists in the determination of the unknown coupling functions q^{te}, q^{tm}, ρ_{mn}, and ρ_{10}. Several solutions have already been proposed [32]. In the present case, we transform the continuity equations into a system of coupled integral equations taking into account the orthogonality properties of the modes on both sides of the discontinuity. These coupled integral equations can be solved by means of an iterative method using Neumann series [32].

Nevertheless, considering realistic approximations of the present problem (with a lossy material in part 2) [31], the zero-order solutions of the Neumann series can accurately describe the near-field phenomena. Consequently, the zero-order solutions make possible an analytical determination of the coupling coefficients, i.e.,

$$q_{(pq)}^{te}=\frac{\beta_{10}|\gamma_2|}{|\gamma_2|^2+\beta_{10}(\beta_2+j\alpha_2)}\langle H_{pq}^{te}|E_y^{10}\rangle \quad (25)$$

$$q_{(pq)}^{tm}=\frac{\beta_{10}|\gamma_2||\epsilon_2^*|}{(\epsilon_2'+j\epsilon_2'')(\beta_{10}\gamma_2+k_0^2\epsilon_2^*)}\langle H_{pq}^{tm}|E_y^{10}\rangle \quad (26)$$

$$\rho_{10}=\frac{1}{4}\int\int_0^\infty q^{te}(pq)\frac{\gamma_2}{|\gamma_2|^2}[\beta_{10}-\gamma_2]\langle H_{pq}^{te}|E_y^{10}\rangle\,dp\,dq+\frac{1}{4}\int\int_0^\infty q^{tm}(pq)\frac{(\beta_{10}\gamma_2-k_0^2\epsilon_2^*)}{k_0^2(\epsilon_2'+j\epsilon_2'')}\langle H_{pq}^{tm}|E_y^{10}\rangle\,dp\,dq \quad (27)$$

where β_{10} is the phase constant of the fundamental incident TE_{10} mode.

Another equation can be added, which represents the energy conservation condition at the discontinuity, and allows us to test the modal method, i.e.,

$$1=|\rho_{10}|^2+\int\int_0^\infty\left[|q^{te}(pq)|^2R(P(pq))+|q^{tm}(pq)|^2R(P(pq))\right]dp\,dq. \quad (28)$$

3) Fields in Lossy Region: Once the analytical determination of the coupling functions $q^{te}(p,q)$ and $q^{tm}(p,q)$ is completed and once modes on both sides of the discontinuity are tabulated, we get the following expressions of the components of the electric field:

$$E_x(x,y,z)=\int\int_0^\infty\left[q^{te}(pq)E_x^{te}(pq)+q^{tm}(pq)E_x^{tm}(pq)\right]e^{-j\gamma_2 z}\,dp\,dq \quad (29)$$

$$E_y(x,y,z)=\int\int_0^\infty\left[q^{te}(pq)E_y^{te}(pq)+q^{tm}(pq)E_y^{tm}(pq)\right]e^{-j\gamma_2 z}\,dp\,dq \quad (30)$$

$$E_z(x,y,z)=\int\int_0^\infty q^{tm}(pq)E_z^{tm}(pq)e^{-j\gamma_2 z}\,dp\,dq. \quad (31)$$

Note that these quantities, combined with the conductivity, will allow the determination of the radiometric weighting functions C_i and C_i' (relations (8) and (12)) at any point in the lossy material.

IV. Preliminary Verifications of Numerical Results

A. Energy Balance in the Plane of Discontinuity

This test is carried out by means of relation (28), which expresses the conservation of energy in the plane of the discontinuity.

TABLE I
VERIFICATION OF THE ENERGY BALANCE IN THE PLANE OF THE DISCONTINUITY
(EN* IS THE POWER IN MEDIUM 2 AT $Z = 0$)

ϵ_1 (Waveguide)	Lossy Material		$\epsilon'2$	$\epsilon''2$	F GHz	$1-\lvert\rho_{10}\rvert^2$	EN*	Ecart %
25	High water content tissue	Water	78	13	3	0.878	0.879	0.1
		Muscle	46	12	3	0.943	0.943	< 0.1
25	Low water content tissue	Aceton	21.1	15	3	0.993	1.06	6.6
12		Fat tissues	5.5	1	3	0.973	1.13	14

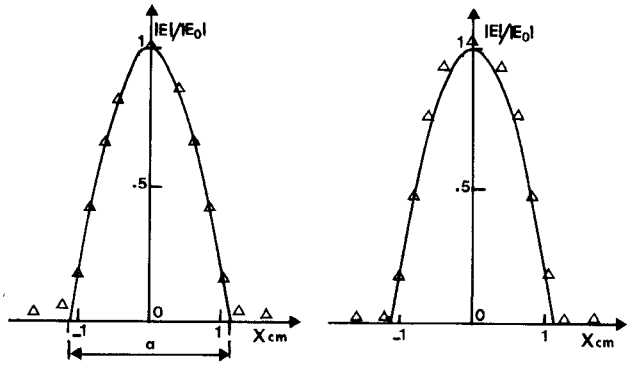

Fig. 4. Verification of the linking up of the electric field in the discontinuity plane: ——— field in the waveguide at $Z = 0$; △ △ field in the semi-infinite medium at $Z = 0$. (a) Muscle tissue ($\epsilon_2' = 46$, $\sigma_2 = 2$ S/m). (b) Water ($\epsilon_2' = 77$, $\sigma_2 = 1.85$ S/m). $F = 3$ GHz, $\epsilon_1 = 25$, $Y = 0$, $a = 2b = 22$ mm.

Table I shows examples of computed data. Note that this study is mainly devoted to medical applications. For this reason we have limited our computations to the case of the permittivities of living tissue. The experiments are carried out on usual lossy liquids. However, the conclusions of this paper also have a bearing on any kind of nonmetallic material. In the general case of very lossy materials (such as high-water-content tissues) the power difference between the two sides of the discontinuity is smaller than 1%. This characteristic warrants our hypothesis, in which we neglect the higher order modes in the waveguide. Nevertheless, for low-loss materials, such as low-water-content tissues, the difference in power between the two sides can reach 14%, which means that the higher order modes in the waveguide should be taken into account. This problem is being taken into account at the present time and will be explained in a future paper.

B. Electric Field in the Plane of Discontinuity

We verify the two hypotheses which consist of neglecting the backward-traveling higher order modes in the waveguide and medium 3 (Fig. 3). For this, we have to verify the equality of the fields in the plane of the discontinuity. Parts (a) and (b) of Fig. 4 show such examples of values of the field on both sides of the discontinuity for high-water-content materials. The two sets of values (in the waveguide and in the lossy material) are in quite good agreement.

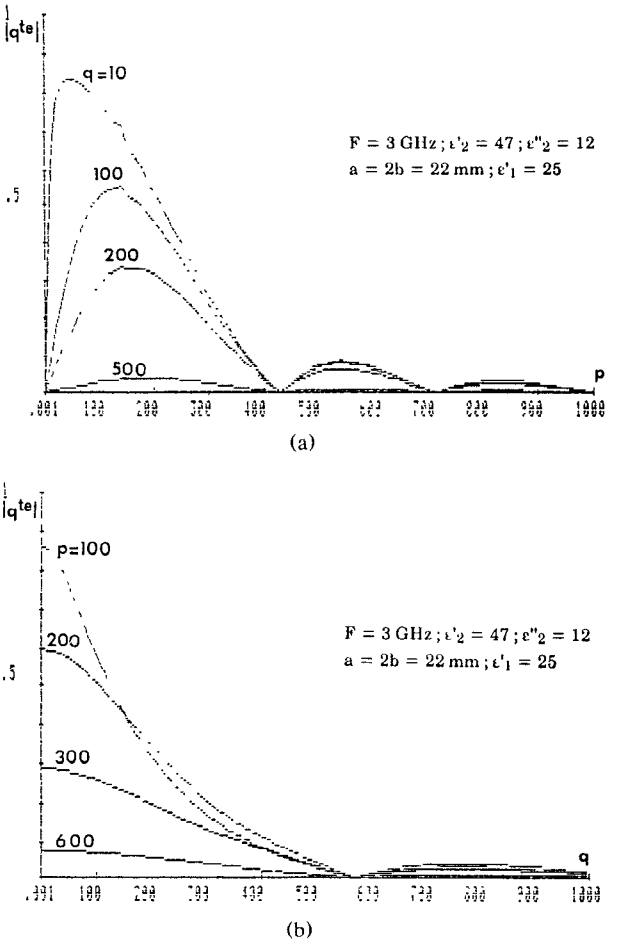

Fig. 5. Coupling functions q^{te} of the modes transmitted in the semi-infinite material (muscle tissue) as a function of the transverse wavenumbers p and q: (a) q^{te} versus p; (b) q^{te} versus q.

C. Numerical Stability

The numerical stability results from the number of continuous modes p and q which are considered and also from the discretization of the domains $(0, p_{max})$ and $(0, q_{max})$, for which the numerical integration leads to expressions (28) to (30). The determination of p_{max} and q_{max} and of the integration steps is arrived at by studying the coupling functions $q^{te}(p, q)$ and $q^{tm}(p, q)$. In Fig. 5 we give an example of the variation of q^{te} versus p and q for high-water-content tissue at 3 GHz. We note that the contribution of the continuous modes can be neglected for p and q greater than 600 m^{-1}. Moreover, the discretization of the integration domain re-

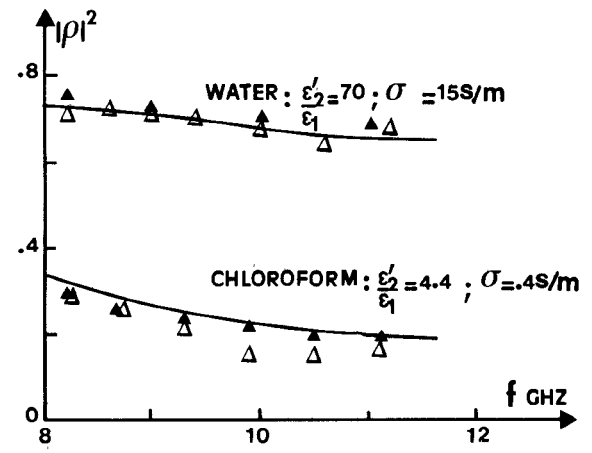

Fig. 6. Comparison between theory and experiment for the reflection coefficient between a rectangular waveguide aperture and water or chloroform: ——— modal method; ▲ ▲ computed [34]; △ △ experiment.

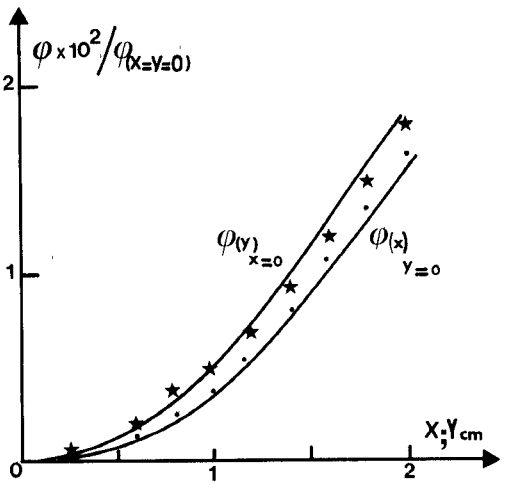

Fig. 8. Field transmitted in water by a waveguide aperture ($a = 2b = 22$ mm, $F = 3$ GHz, $z = 2$ cm). Phase of field versus x and y: ——— modal method; ●⋆ experiment.

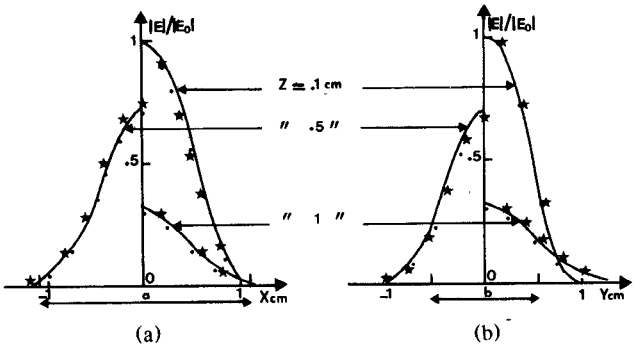

Fig. 7. Field transmitted in water ((a) and (b)) by a waveguide aperture ($a = 2b = 22$ mm; $\epsilon_1 = 16$) at 3.2 GHz: ——— modal method; ●● computed [29]–[34]; ⋆⋆ experiment.

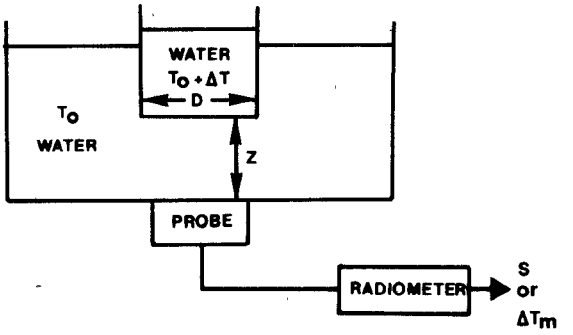

Fig. 9. Physical model used in experiments carried out for compact thermal structures.

sults from the velocity of variations of the functions $q^{te}(p,q)$ and $q^{tm}(p,q)$.

V. Comparison Between Theory and Experiments in the Active Process

In this section, we consider experiments made in the following way. A monochromatic microwave source is connected to the different kinds of probes (waveguide apertures) which are also used in the radiometric experiments. The construction, characteristics, and tests over such probes have been described in previous papers [33], [34]. The waveguide apertures transmit a microwave signal in a homogeneous lossy material.

We first present, in Fig. 6, a comparison between the computed and measured reflection coefficients. A good agreement between our experiments, the present modal method, and previously reported computed data [34] is illustrated.

Other comparisons refer to the field transmitted in the lossy materials. This field mapping is carried out by means of small monopole antennas connected either to a square law detector or to a network analyzer.

We note that a good agreement between our modal method, experiment and methods already published [34] considering that the lossy material fills an oversize waveguide, is obtained. These data, which consider either the amplitude or the phase shift of the field as a function of different geometrical parameters x, y, and z are reported in Figs. 7 and 8.

VI. Experimental Verification of Radiometric Data

We first consider total power radiometry. The physical model which has been considered is shown in Fig. 9. In a semi-infinite homogeneous lossy material at a temperature T_0, a cylindrical structure of the same material, (diameter D) is at a different temperature $T_0 + \Delta T$. The axis of this structure is perpendicular to the interface; the structure is at a distance z from the interface.

The radiometric signals are computed by application of relations (5), (8), and (9), while the values $|E_i(f)|$ are computed by means of the modal method. We have considered the case of water with $T_0 = 33°C$ and $\Delta T = 5°C$. This small value of ΔT allows us to assume the same permittivity at any place in the model regardless of the temperature.

The radiometer working frequencies are 1.5 GHz $\pm$ 0.5 GHz and 3 GHz $\pm$ 0.5 GHz. The corresponding bandwidths are taken into account in the computation. The values of the

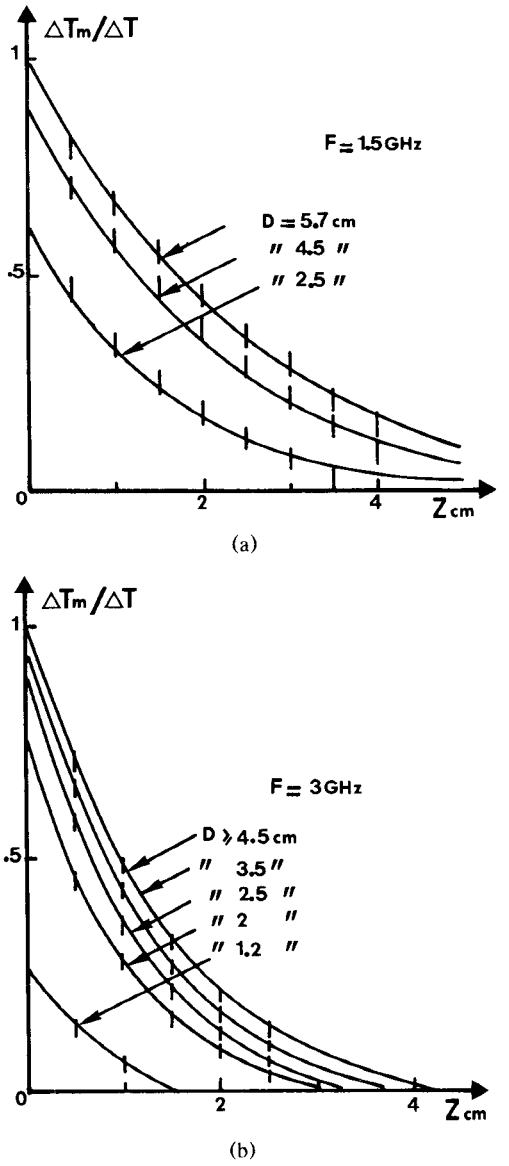

Fig. 10. Radiometric signals in the situation described in Fig. 10 in the case of water: $T_0 = 33°C$, $\Delta T = 5°C$ (probe $\epsilon_1 = 25$, $a = 2b = 22$ mm): modal method; | experiment.

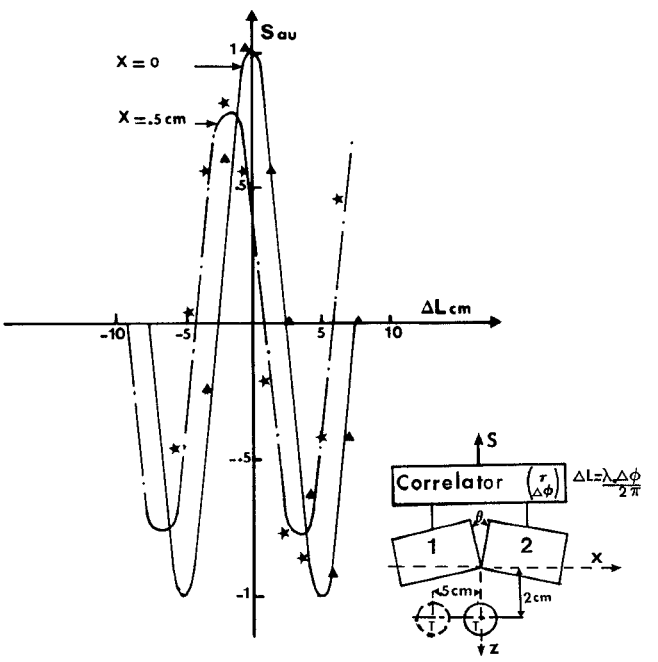

Fig. 11. Signal of a correlation radiometer: for water at $T_0 = 30°C$ the thermal structure ($\Delta T = 19°C$) is a cylinder (diameter $D = 2$ cm) parallel to the line of junction of the probes ($\Theta = 30°$, angle between the axes of observation of the probes): —·° modal method; ▲★ experiment.

permittivity of water are taken from [35]. The same model has been realized in practice and the measurements have been achieved by means of two radiometers having the above frequencies, i.e., 1.5 ± 0.5 GHz and 3 ± 0.5 GHz.

A comparison between computed and experimental data is given in Fig. 10 in terms of the ratio $\Delta T_m / \Delta T$ versus z for different diameters D of the structure. The considered situation is related to the position of the probe facing the center of the thermal structure, i.e., the position of the probe receiving the maximal noise power. We note that the computed values are always within the error margins of the experimental data [6], [31]. Note also the necessity for using a three-dimensional model: such results point out that, for the same value ΔT, the radiometric signal depends both on the depth of the structure and on its size (D in the present case).

Other comparisons between theory and practice are related to correlation radiometry. The correlation radiometer has been described in previous publications [7], [8]; its bandwidth is 2–4 GHz.

Concerning the computations, the coupling parameters C_i' for the different subvolumes ΔV_i have been defined in relation (12). Consequently for a lossy material at a temperature T_0' in which a volume V is at a temperature $T_0' + \Delta T$ and for a small bandwidth near the frequency f we get an output signal

$$S(f,\tau) = G'(f) \sum_{i=1}^{\infty} C_i'(f,\tau) T_i \tag{32}$$

$$S(f,\tau) = G'(f) \left[\sum_{i \in V} C_i'(f,\tau)(T_0' + \Delta T) + \sum_{i \notin V} C_i'(f,\tau) T_0' \right] \tag{33}$$

$$S(f,\tau) = G'(f) \left[\sum_{i \in V} C_i'(f,\tau) \Delta T + \sum_{i=1}^{\infty} C_i'(f,\tau) T_0' \right]. \tag{34}$$

A consequence of the principle of detailed balancing [22] is that our correlator radiometer output signal is zero when the temperature of the lossy material is uniform [7]. Hence, the expression for the output signal reduces to

$$S(f,\tau) = G'(f) \sum_{i \in V} C_i'(f,\tau) \Delta T. \tag{35}$$

A comparison between theoretical and experimental values of $S(f,\tau)$ is related to the different kinds of thermal structures in water. In Fig. 11, we consider a cylinder whose axis is parallel to the line of junction of the two probes. The signal, given as a function of the delay $\Delta L = 2C\tau$, corresponds to two positions of the thermal structure ($X = 0$ and $X = 0.5$ cm).

In Fig. 12, we consider that a plane surface, parallel to the plane of symmetry of the two probes, defines two parts of the

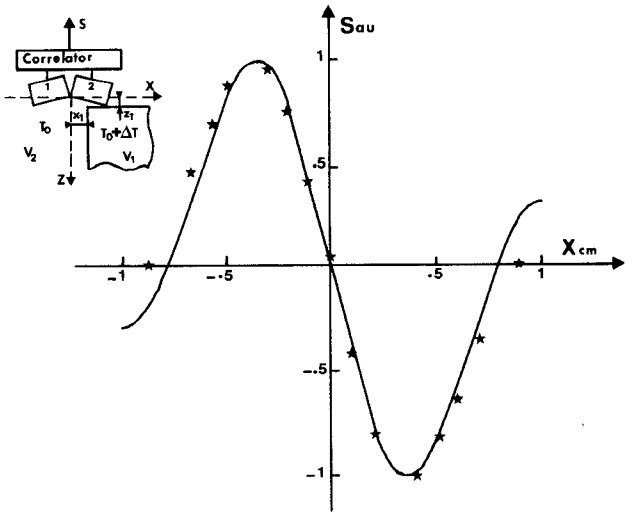

Fig. 12. Signal of a correlation radiometer: case of water: two parts respectively at $T_0 = 20°C$ and $T_0 + \Delta T$ ($\Delta T = 5°C$) are separated by a plane area parallel to the plane of symmetry of the probes ($\Theta = 30°$, $Z_1 = 5$ mm), $\tau = 0$: ——— modal method; ★★ experiment.

lossy material, one being at a temperature T_0 and the other at $T_0 + \Delta T$. Fig. 12 refers to the output signal as a function of position X_1 of the area limiting the two parts of the material at T_0 and $T_0 + \Delta T$.

In all these situations, we observe quite a good agreement between the results of the radiometric data, as deduced from the modal method explained in this paper, and the experiments. Note also that correlation radiometry is particularly able to detect a small variation of the position of a thermal structure either by a modification of the position of the double probe or by action on the delay time τ.

VII. Conclusion

We have developed a method for computing of the near field transmitted by a monomode rectangular waveguide aperture into a homogeneous lossy material. This method has been applied to the computation of radiometric signals for both total power and correlation radiometry. Following preliminary verifications, comparison of the radiometric with experimental data points out quite a good agreement in the case of models made of water near 1.5 and 3 GHz. Consequently, this method of computing the radiometric signals can now be used for medical applications, in which high-water-content tissues often correspond to practical situations [36].

References

[1] A. H. Barret, P. C. Myers, and N. L. Sadowski, "Detection of breast cancer by microwave radiometry," *Radioscience*, vol. 12, pp. 167–171, 1977.
[2] L. Enel, Y. Leroy, J. C. Van de Velde, and A. Mamouni, "Improved recognition of thermal structures by microwave radiometry," *Electron. Lett.*, vol. 20, Mar. 1984.
[3] K. L. Carr, A. El-Mahdi, and J. Shaeffer, "Dual-mode microwave system to enhance early detection of cancer," *IEEE Trans. Microwave Theory Tech.*, vol. MTT-29, Mar. 1981.
[4] D. V. Land, "Radiometer receivers for microwave thermography," *Microwave J.*, vol. 26, no. 5, 1983.
[5] S. Mizushina, Y. Hamamura, and T. Siguera, "Three band microwave radiometer system for noninvasive measurement of the temperature at various depths," in *IEEE MTT-S Int. Microwave Symp. Dig.*, 1986, pp. 759–762.
[6] Y. Leroy, A. Mamouni, J. C. Van de Velde, B. Bocquet, and B. Dujardin, "Microwave radiometry for noninvasive thermometry," *Automedica*, vol. 8, pp. 181–202, 1987.
[7] A. Mamouni, Y. Leroy, J. C. Van de Velde, and L. Bellarbi, "Introduction to correlation microwave thermography," *J. Microwave Power*, vol. 18, no. 3, pp. 285–293, 1983.
[8] L. Bellarbi, A. Mamouni, J. C. Van de Velde, and Y. Leroy, "Accurate localisation of thermal gradients in lossy materials by correlation microwave thermography," *Electron. Lett.*, vol. 20, no. 10, 1984.
[9] J. C. Hill and R. B. Goldner, "The thermal and spatial resolution of a broad band correlation radiometer," *IEEE Trans. Microwave Theory Tech.*, vol. MTT-33, pp. 718–722, 1985.
[10] N. H. Haslam, A. R. Gillespie, and C. G. T. Haslam, "Aperture synthesis thermography. A new approach to passive microwave temperature measurements in the body," *IEEE Trans. Microwave Theory Tech.*, vol. MTT-32, 1984.
[11] G. Schaller, "Synthetic aperture radiometry for imaging of hot spot in tissue," *Proc. 17th European Microwave Conf.* (Roma), 1987.
[12] G. Giaux *et al.*, "Microwave imaging at 3 GHz for the exploration of tumors of the breast," in *IEEE MTT-S Int. Microwave Symp. Dig.*, 1988.
[13] D. D. Nguyen, A. Mamouni, Y. Leroy, and E. Constant, "Simultaneous microwave local heating and microwave thermography. Possible clinical applications," *J. Microwave Power*, vol. 14, pp. 135–137, 1979.
[14] D. D. Nguyen, M. Chivé, Y. Leroy, and E. Constant, "Combination of local heating and radiometry by microwaves," *IEEE Trans. Instrum. Meas.*, vol. IM-29, pp. 143–144, 1980.
[15] G. Giaux, B. Prévost, Y. Leroy, M. Chivé and M. Plancot, "Local hyperthermia of cancers, by radiofrequency or microwaves, in combination with radiotherapy or chemotherapy controlled by microwave thermography: Technical aspects; first clinical observations," presented at Fourth European Hypert. Meeting, London, July 1982.
[16] J. Conway, Univ. Sheffield, U.K., personal communication.
[17] F. Bardati, M. Mongiardo, and D. Solimini, "Inversion of microwave thermographic data by the singular function method," in *IEEE MTT-S Int. Microwave Symp. Dig.*, 1985, pp. 75–77.
[18] B. Bocquet, A. Mamouni, M. Hochedez, J. C. Van de Velde, and Y. Leroy, "Visibility of local thermal structures and temperature retrieval by microwave radiometry," *Electron. Lett.*, vol. 22, no. 3, pp. 120–122, 1986.
[19] B. Bocquet, A. Mamouni, J. C. Van de Velde, and Y. Leroy, "Imagerie thermique par radiométrie microonde," *Rev. Phys. Appl.*, vol. 23, pp. 1273–1279, 1988.
[20] R. H. Dicke, "The measurement of thermal radiation at microwave frequencies," *Rev. Sci. Instr.*, vol. 17, no. 7, 1946.
[21] A. Stogryn, "The brightness temperature of vertically structure medium," *Radio Sci.*, vol. 5, no. 12, 1970.
[22] H. Bosma, "On the theory of linear noisy systems," N. V. Philips Gloeilamen Fabriken, Eindhoven, 1967.
[23] A. T. Dehoop and G. Dejong, "Power reciprocity in antenna theory," *Proc. Inst. Elec. Eng.*, vol. 121, no. 3, 1974.
[24] A. W. Guy, "Electromagnetic fields and relative heating patterns due to a rectangular aperture source in direct contact with bilayered biological tissue," *IEEE Trans. Microwave Theory Tech.*, vol. MTT-19, no. 2, 1971.
[25] A. T. Villeneuve, "Admittance of waveguide radiating into plasma environment," *IEEE Trans. Antennas Propagat.*, vol. AP-18, no. 2, 1970.
[26] R. F. Harrington, *Time-Harmonic Electromagnetic Fields*. New York: McGraw-Hill, 1961.
[27] F. Bardati, M. Mougiardo, D. Solimini, and P. Tognalatti, "Biological temperature retrieval by scanning radiometry," in *IEEE MTT-S Int. Microwave Symp. Dig.*, 1986, pp. 763–766.
[28] E. Cheever, J. B. Leonard, and K. R. Foster, "Depth of penetration of fields from rectangular apertures into lossy media," *IEEE Trans. Microwave Theory Tech.*, vol. MTT-35, no. 9, 1987.
[29] J. Audet *et al.*, "Electrical characteristics of waveguide applicators for medical applications," *J. Microwave Power*, vol. 15, pp. 177–186, 1980.

[30] J. A. Encinar and J. M. Rebollar, "Convergence of numerical solutions of open-ended waveguide by modal analysis and hybrid modal-spectral techniques," in *IEEE MTT-S Int. Microwave Symp. Dig.*, 1985, pp. 575–578.
[31] A. Mamouni, "Radiometrie microonde en champ proche," Thèse de doctorat d'Etat, Lille, 1988.
[32] Ph. Gelin, "Traitement électromagnétique des discontinuités en guides d'ondes diélectriques," Thèse de doctorat d'Etat, Lille, 1981.
[33] D. D. Nguyen *et al.*, "Microwave thermography: The modeling of probes an approach toward thermal pattern recognition," in *Proc. 10th European Microwave Conf.* (Warsaw), 1980.
[34] J. Audet, "Etude numérique et expérimentale de discontinuités entre guides d'ondes," Thèse de 3e cycle, Paris-Sud, 1980.
[35] F. Buckley and A. A. Maryott, "Tables of dielectric dispersion data for pure liquids and dilute solutions," Washington, 1957.
[36] B. Bocquet, J. C. Van de Velde, A. Mamouni et al. "Microwave radiometric imaging at 3 GHz for the exploration of breast tumors," *IEEE Trans. Microwave Theory Tech.*, vol. 38, pp. 791–793, June 1990.

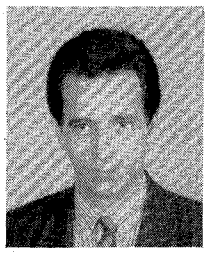

Ahmed Mamouni was born in 1949 in Morroco. He received the These de Doctorat d'Etat (electronics) from the Université des Sciences et Techniques de Lille Flandres Artois, France, in 1988.

Presently, he is Assistant Professor of Electrical Engineering at this university and is working in the Centre Hyperfréquences et Semiconducteurs there on new applications of microwaves for systems and sensors that can be used in biomedical engineering and industry. Since 1985, his main interest has been the computation of near-field microwave radiometric signals and the inversion of these signals.

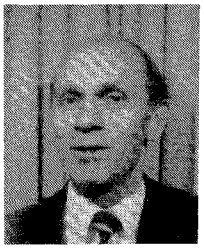

Yves Leroy received the These de Doctorat d'Etat (electronics) from the Université des Sciences et Techniques de Lille, France, in 1967.

He became a Professor at this university in 1970 and worked in the Centre Hyperfréquences et Semiconducteurs there on weak field and hot carrier transport phonomena in semiconductors. He has been manager of the research group since 1976. His work has focused on new applications of microwaves, leading to the definition and industrial development of systems and sensors for biomedical engineering (radiometric imaging, hyperthermia controlled by radiometry) and industry.

Dr. Leroy is the author of 165 publications and communications, the holder of six patents, and the coauthor of several parts of books dealing with applications of microwaves.

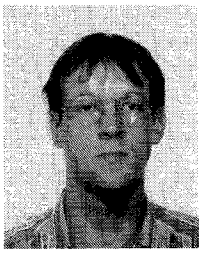

Bertrand Bocquet was born in La Bassée, France, on May 17, 1960. He received the Thèse d'Université (electronics) from the Université des Sciences et Techniques de Lille Flandres Artois, France, in 1989.

Presently, he is an Assistant Professor at this university and is with the Centre Hyperfréquences et Semiconducteurs there working on applications of microwave radiometric imaging, in particular for the diagnosis of breast cancer.

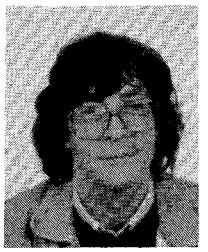

J. C. van de Velde was born in Lille, France, on February 28, 1948. He received the Diploma degree in electrical engineering from the Centre National des Arts et Métiers of Lille, France, in 1980.

Since then he has been involved in research on new applications microwaves for medicine and for sensors devoted to transport and industrial applications. Mr. van de Velde is the holder of six patents.

Philippe Gelin (A'87) was born on June 1, 1948, in St. Avold, France. He received the doctor in physics degree from the Technical University of Lille, France, in 1981.

Presently, he is Professor of Electrical Engineering at the Ecole Nationale Supérieure des Télécommunications de Bretagne, Brest, in the Laboratoire d'Etudes des Systèmes de Télécommunications (LEST, URA CNRS no. 723).